



Isolation and structural characterization of degradation products of afatinib dimaleate by LC-Q-TOF/MS/MS and NMR: cytotoxicity evaluation of afatinib and isolated degradation products

Balasaheb B. Chavan^a, Sawant Vitthal^a, Roshan M. Borkar^b, Ragampeta Srinivas^{a,b}, M.V.N. Kumar Talluri^{a,*}

^a Department of Pharmaceutical Analysis, National Institute of Pharmaceutical Education & Research, IDPL R&D Campus, Balanagar, Hyderabad- 500 037, India

^b National Center for Mass Spectrometry, CSIR-Indian Institute of Chemical Technology, Tarnaka, Hyderabad 500 607, India



ARTICLE INFO

Article history:

Received 24 August 2018

Received in revised form 1 January 2019

Accepted 5 January 2019

Available online 7 January 2019

Keywords:

Afatinib

Stress degradation

Degradation products

LC-Q-TOF/MS/MS

NMR

In silico toxicity

ABSTRACT

Afatinib is an irreversible tyrosine kinase receptor inhibitor which was approved lately by USFDA for the treatment of metastatic non-small cell lung cancer (NSCLC). AFT was subjected to stress degradation studies under hydrolytic (acid, base and neutral), oxidative, thermal and photolytic conditions to investigate the inherent stability of the drug. The present study describes the simple and rapid HPLC method development for the selective separation of the AFT and its degradation products. The drug and degradation products were separated on Agilent Eclipse plus C18 (150 × 4.6 mm, 5 μ) column with ammonium acetate buffer (10 mM, pH 6.7) in gradient elution mode. The drug was found to be unstable in all the conditions studied. The developed chromatographic method was extended to tandem mass spectrometry (QTOF-MS) for the characterization of the degradation products. A total of 11 unknown degradation products were characterized using liquid chromatography quadrupole time-of-flight mass spectrometry (LC-Q-TOF/MS/MS). Two major degradation products (DP2 and DP3) were isolated using preparative HPLC and their structures were confirmed by conducting ¹H and ¹³C NMR experiments. The isolated DPs were evaluated for their anticancer potential using non small cell lung cancer cell line A549. The IC₅₀ values for AFT, DP2 and DP3 were found to be 15.02 ± 1.49, 25.00 ± 1.26 and 32.56 ± 0.11 respectively. The *in silico* toxicity studies were performed employing ProTox-II software for the assessment of toxicity potential of drug and its degradation products. Finally, the developed chromatographic method was validated as per the International Conference on Harmonization guideline Q2 (R1).

© 2019 Published by Elsevier B.V.

1. Introduction

Afatinib diamaleate (AFT) ([N-[4-[(3-chloro-4-fluorophenyl)amino]-7-[(3S)-tetrahydro-3-furanyl]oxy]-6-quinazolinyl]-4(dimethylamino)-2-butenamide]) an anilinoquinazoline derivative is an irreversible tyrosine kinase receptor inhibitor used in the therapy of metastatic non-small cell lung cancer (NSCLC) which is the common type of lung cancer [1]. Afatinib selectively and irreversibly binds and inhibits the epidermal growth factor receptors and certain epidermal growth factor receptor (EGFR) mutants which result in the inhibition of tumor growth and angiogenesis in tumor cells [2]. Recently, the Food

and Drug Administration granted approval to AFT for a broadened indication in first-line treatment of patients with metastatic non-small cell lung cancer (NSCLC) whose tumors have non-resistant EGFR mutations as detected by an FDA-approved test. The most common adverse reactions reported for AFT across clinical trials are diarrhea, rash/acne dermatitis which varies with individuals [3].

Stress stability studies of drug substances and drug products are important part of drug development process and primarily used to forecast drug stability. Stability studies can be useful in selection of storage conditions, packaging materials and handling. In addition these studies help to identify the degradation products, in turn aid in establishing the degradation pathways and inherent stability of the molecule. Thus, as per regulatory guidelines forced degradation studies and characterization of formed degradation products (DPs) or impurities at or above 0.1% should be carried out in drug substance [4,5].

* Corresponding author.

E-mail addresses: narendra.talluri@gmail.com, [\(M.V.N.K. Talluri\).](mailto:narendra@niperhyd.ac.in)

A thorough literature search revealed that, few reports are available in the literature about the liquid chromatographic tandem mass spectrometric method for the determination of AFT in animals [6] and humans [7]. Also, liquid chromatographic determination of several tyrosine kinase inhibitors including AFT was reported using diode array detection [8,9]. In addition, pharmacokinetic [10] and metabolism studies [11] of the drug in humans has been reported. Very few reports are present on determination of drug in bulk and dosage forms [12]. To the best of our knowledge, there are no reports which explain the stability indicating HPLC method development and comprehensive forced degradation studies of AFT using LC-Q-TOF/MS/MS and NMR. Over the last decade Liquid chromatography-tandem mass spectrometry (LC-MS/MS) in combination with high resolution and NMR has been widely utilized for the identification and characterization of forced degradation products (DPs) [13–16]. The *in vitro* studies were carried out to check the cytotoxicity of isolated DPs by MTT assay using A549 cell line. The *in silico* toxicity studies is a useful tool for the prediction of toxicities of the molecules. In the present study, the *in silico* toxicity studies were carried out using ProTox-II software, to assess the toxicological potential of the drug and DPs, which can be useful to develop safer analogues.

Hence, the aim of present study was to investigate degradation behavior of the drug which includes: (i) to carry out stress degradation studies (hydrolytic, oxidative, thermal and photolytic) according to ICH prescribed guideline Q1A (R2) [4], (ii) development of HPLC method for selective separation of drug and its DPs, (iii) isolate the major DPs (DP2 and DP3) by preparative HPLC, (iv) characterize the DPs using LC-MS/MS and NMR (v) *in vitro* toxicity evaluation of DP2 and DP3 by MTT assay (vi) *in silico* toxicity assessment of drug and its DPs using ProTox-II software and (vii) validation of the developed HPLC method as per ICH guideline [17].

2. Experimental

2.1. Chemicals and reagents

AFT was obtained as a gratis sample from Sun Pharmaceutical Industries Ltd. Vadodara, Gujarat, India. LC-MS CHROMASOLV® grade acetonitrile (ACN) were procured from Sigma-Aldrich (Bangalore, India). Analytical reagent grade Ammonium acetate, ammonium formate, formic acid, hydrochloric acid (HCl), sodium hydroxide (NaOH) and acetic acid were purchased from SD Fine Chemicals (Mumbai, India). Methanol (MeOH) and acetonitrile (ACN) were procured from Sigma-Aldrich (Bangalore, India). AR grade hydrogen peroxide (H_2O_2) was purchased from Merck (Mumbai, India). HPLC grade water was used for the preparation of all the samples and buffer which was obtained from Evoqua Integrated Ultra Care TW GP Water purification system (United States). Tetramethylsilane (TMS) and DMSO were purchased from Sigma-Aldrich (Bangalore, India) and Cambridge Isotope Laboratories, Inc. Andover (MA, USA), respectively. The (3-(4,5-Dimethylthiazol-2-Yl)-2,5-Diphenyltetrazolium Bromide (MTT) reagent was obtained from Hi Media (Hyderabad, India). Non small cell lung cancer cell line A549 line was procured from NCCS (Pune, India).

2.2. LC separation of AFT and DPs

Chromatographic separation of AFT and DPs were achieved on Agilent Eclipse plus C18 (150 × 4.6 mm, 5 μ) column with 10 mM ammonium acetate (pH 6.7) as solvent A and ACN as solvent B using the following linear gradient: 0 min 10% B; 5 min 50% B, 7 min 80% B, 10 min 80% B, 11 min 10% B and 12 min 10% B using a Waters 2695 series HPLC system (M.A, USA) equipped with auto sampler, quaternary gradient pump, in-line degasser, column compartment with

temperature control unit and photo diode array (PDA) detector. Empower 3 software was used for the collection of data. The flow rate of the mobile phase and injection volume were optimized at 1 mL min^{-1} and 5 μL , respectively. The column was equilibrated with mobile phase for 10 min. prior to sample injection.

LC-MS experiments were carried out on Agilent 1200 series (Agilent technologies, USA) attached to quadruple-time of flight (Q-TOF LC/MS 6540 series, Agilent Technologies, USA) where ESI was used as ionization source in positive scan mode. Mass Hunter Workstation software was used for data acquisition. Typical mass operating source conditions were optimized as fragmentation voltage was 170 V, capillary voltage at 3500 V, capillary temperature 250 °C, skimmer voltage at 60 V. Nitrogen was used as the drying (350 °C, 10 L min^{-1}) and the nebulizing gas at pressure 45 psi.

The ^1H and ^{13}C NMR experiments were conducted using a 500 MHz NMR (AVANCE III HD 500, Bruker, Switzerland) spectrometer. TMS and deuterated DMSO were used as an internal standard and solvent for the NMR experiments, respectively. The chemical shift values were reported on the δ scale in ppm.

2.3. Stress degradation study

Stress degradation studies were carried out as per the ICH Q1 A (R2) guideline. The degradation studies were carried out at 1000 $\mu\text{g mL}^{-1}$ concentration. The degradation samples were collected at regular intervals to check the formation of DPs. Hydrolytic degradation studies were carried out in acid, base and neutral conditions. Alongside oxidative, thermal and photolytic stress degradation studies were performed. The drug was found to be degraded under hydrolytic, oxidative, photolytic and thermal condition. The acidic, basic and neutral degradation was executed by reflux heating of the AFT in 1 N HCl, 0.02 N NaOH and water at 80 °C, respectively. The oxidation of the drug was investigated in 30% of H_2O_2 for 3 days. Photolytic forced degradation studies were performed to investigate the effect of UV and fluorescence light on the drug using a photostability chamber (Newtronic life care sciences equipment Pvt. Ltd. India) equipped with an illumination bank made of light source as described in the ICH guideline Q1B [18]. The thermal degradation studies were performed in a hot air oven (Oswarld scientific Pvt. Ltd. India, model no. 00GS S-90) where the drug was kept in the petri plate as a thin layer. The photostability studies were conducted in solid as well as in liquid form in photostability chamber by exposing total dose of 200 W h m^{-2} of UV light and 1.2×10^6 lux h of fluorescence light at 40 °C and 75%RH. Alongside set of the control samples were stored in dark at the same temperature to serve as control.

2.4. Sample preparation

Stock solution of AFT (1000 $\mu\text{g mL}^{-1}$) was prepared by dissolving the drug in diluent (water: ACN 50:50 v/v). The stock solution was further diluted for the preparation working standard (200 $\mu\text{g mL}^{-1}$). Acidic and basic samples were neutralized with appropriate strengths of base and acid respectively before injecting the sample. All the degradation samples were filtered through 0.22 μm nylon membrane syringe filter before subjected to HPLC and LC-MS/MS analysis and analyzed at 200 $\mu\text{g mL}^{-1}$ concentrations.

2.5. Isolation of DPs by preparative HPLC

The developed chromatographic method was transferred from analytical HPLC to preparative HPLC for isolation of the DPs. The preparative isolation of the major degradation products was carried out on a preparative HPLC from Waters (Milford, MA, USA) equipped with 515 HPLC pumps and 2489 UV-vis detectors. The separation and isolation of the DPs (DP2 and DP3) was carried out

on a Waters X bridge C18 column ($250 \times 19 \text{ mm} \times 5 \mu\text{m}$, 130 \AA). The mobile phase used was solvent-A ammonium acetate (pH 6.7; 10 mM) with solvent-B ACN as organic solvent in gradient elution mode set as 0/10, 6/50, 9/80, 13/80, 15/10, 16/10, 18/10 (Time min/% solvent B). The flow rate and injection volume was 10 mL min^{-1} and 1 mL, respectively. The wavelength for identification of DPs was fixed at 258 nm. The DP2 and DP3 were isolated for structural confirmation by NMR. The drug (1000 mg mL^{-1}) was allowed to degrade in 0.5 N NaOH and 3 N HCl solution for 4 h to get a higher percentage of the DP2 and DP3, respectively. The degraded solutions of acidic and basic degradation were neutralized with the appropriate concentrations of NaOH and HCl, respectively. The fraction of DPs were collected by multiple injections into preparative HPLC and pooled together. Pooled fractions were concentrated at 35°C using a rotary evaporator to remove ACN and further lyophilized to get the solid compound. The isolated DPs were found to be pure with chromatographic purity $>98\%$. The solid form of the DPs was dissolved in DMSO and submitted for NMR analysis.

2.6. In vitro cell viability assay

The effect of AFT and its DPs (DP2 and DP3) on viability of non small cell lung cancer cell line A549 was evaluated using MTT assay. Briefly, 5×10^3 cells per well were seeded in 96-well plate. After 24 h, cells were treated with AFT, DP2 and DP3 at suitable concentrations in respective wells (highest concentration $40 \mu\text{M}$). Post treatment (48 h), media was aspirated and $100 \mu\text{L}$ of MTT solution was added at a final concentration of 0.5 mg mL^{-1} followed by incubation for 4 h. Then, MTT solution was discarded and $200 \mu\text{L}$ of DMSO was added to dissolve the formazan crystals and incubated for 30 min. Absorbance was measured at 570 nm with a multi-mode spectrophotometer (Molecular devices, USA). Experiments were performed in triplicates and data was expressed as percentage cell viability versus concentration of the compound by taking control cells as 100% viable cells.

3. Results and discussion

3.1. Validation of the HPLC method

The developed HPLC method for AFT was validated according to the ICH recommended guidelines Q2 (R1). The specificity of the method was evaluated by the purity angle and purity threshold values of the peaks by PDA detector. The peak purity assessment shows that purity angle of AFT was found to be less than the purity threshold in presence of all the DPs suggests the purity of the peak. The limit of detection (LOD) and limit of quantification (LOQ) indicates the concentration of the drug where signal to noise (S/N) ratio would be 3 and 10, respectively. The LOD and LOQ for AFT were found to be 3 and $7 \mu\text{g mL}^{-1}$. The linearity of the developed method was determined by plotting calibration curve using standard solution of the drug at eight different concentrations (triplicate) in the range of $10\text{--}350 \mu\text{g mL}^{-1}$. Standard calibration curve were plotted by taking average peak area of each concentration. The data was subjected to statistical analysis using linear regression model. The linear regression equation and correlation coefficient (r^2) were $y = 11352x + 54,857$ and 0.999 , respectively. The data shows good linearity. Accuracy of the developed HPLC method was determined by standard addition method. Standard drug (AFT) at three different concentration levels (80, 100 and 120%) were added into the sample solutions and analyzed in triplicate ($n = 3$). The percentage recovery of the drug was calculated by comparison of the peak area values of test samples with standard drug solutions. The percentage recovery ranged and relative standard deviation (RSD) values were found to be 99.58–100.48% and within 1%, respectively

(Table S1). The precision of the method was studied as repeatability and inter day precision. Repeatability is expressed over short interval of time and also termed as intraday precision. The repeatability of the drug was determined at 100% of the test concentration ($200 \mu\text{g mL}^{-1}$) using six determinations and assay value obtained was expressed in terms of % RSD. The % RSD value was found to be less than 1%, indicating repeatability of the method. The inter day precision expresses inter day variation on different days and evaluated for three consecutive days at the assay concentration ($200 \mu\text{g mL}^{-1}$). The results of the study were expressed as % RSD values and at each day RSD values were below 2%, indicate precision of the method (Table S2). The robustness of the method was determined by deliberate change in certain method parameters like pH of mobile phase (6.7 ± 0.2), flow rate ($1.0 \pm 0.2 \text{ mL min}^{-1}$), column temperature ($25 \pm 5^\circ\text{C}$). No significant change was found in the assay value of the AFT which indicates the robustness of the method.

3.2. Stability indicating method of AFT

AFT was studied and found to be susceptible under all studied forced degradation conditions (hydrolytic, oxidative, photolytic and thermal) with optimized conditions reported in Table S3. A total of 11 DPs were formed under the various stress conditions and were separated chromatographically (Fig. 1) and were characterized by ESI/QTOF MS/MS, with the proposed structures shown in Scheme 1 and 2. Extracted UV spectra of drug and DPs are shown in Fig. S1 and Fig. S2.

3.2.1. Hydrolytic degradation

Acid hydrolysis was performed using 1 N HCl (4 h at 80°C) where optimum degradation of the AFT was found (DP1, DP2 and DP3) (Fig. 1b). Excess degradation was observed when AFT was refluxed with 1 N NaOH . At 0.02 N NaOH for 4 h at 80°C , DP2, DP3 and DP4 were formed (Fig. 1c). For neutral degradation study, the drug was refluxed for 24 h at 80°C in diluent. The drug was degraded to form four DPs (DP1, DP2, DP3 and DP5) (Fig. 1d).

3.2.2. Oxidative degradation

The oxidative degradation study results in the formation of DP1 and DP6 in 30% H_2O_2 after 3 days (Fig. 1e).

3.2.3. Thermal and photolytic degradation

AFT was found to be degraded after 2 days at 80°C and showed formation of DP2, DP5 and DP7 (Fig. 1f). Photolytic degradation of AFT was observed in solid state with four DPs (DP2, DP8, DP9 and DP10) and liquid state with three DPs (DP2, DP9 and DP11) (Fig. 1g-j).

3.3. LC-ESI-Q-TOF/MS/MS and NMR studies of AFT dimaleate and its DPs

Structural elucidation of all the DPs formed under various stress conditions was carried out with the help of LC/ESI-Q-TOF-MS/MS experiments. The most probable structures for the DPs were proposed based on the MS/MS fragmentation pattern of the drug and DPs. The elemental composition of the AFT and protonated DPs along with product ions formed are provided in Table 1. The elemental composition of all the product ions of drug and DPs along with the mass error has been provided in the Table S4. The MS/MS fragmentation patterns for the drug and degradation products are given in Fig. S3-S5. Further, major DPs (DP2 and DP3) were isolated for the structural confirmation by NMR studies.

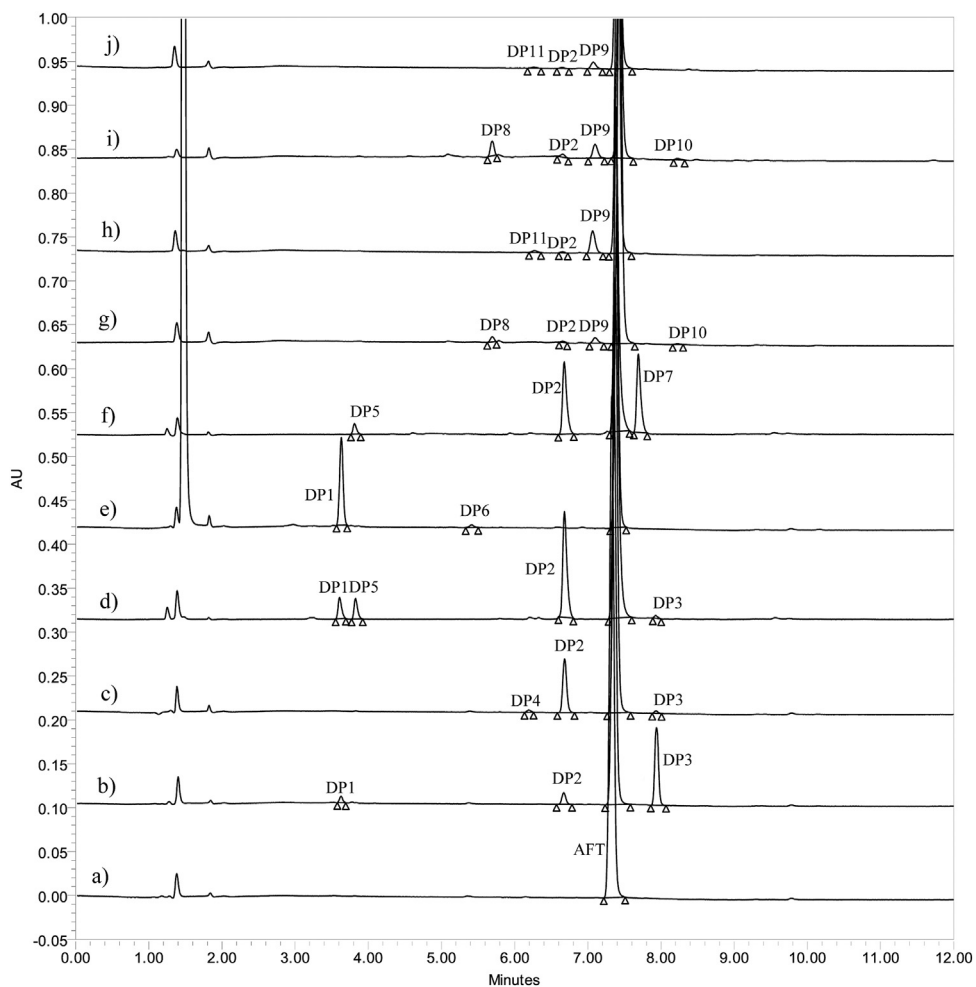


Fig. 1. The overlay of HPLC chromatogram of (a) AFT (b) acidic (c) basic (d) neutral (e) oxidation (f) thermal (g) UV solid (h) UV liquid (i) fluorescence solid (j) fluorescence liquid conditions.

Table 1
Elemental composition of afatinib (AFT) and its degradation products (DP1–DP11).

AFT and its DPs	Molecular Formula	Calculated <i>m/z</i>	Observed <i>m/z</i>	Error (ppm)	MS/MS fragment ions
AFT	C ₂₄ H ₂₆ ClFN ₅ O ₃ ⁺	486.1703	486.1700	-0.62	441, 429, 416, 398, 375, 371, 359, 343, 331, 317, 305, 288, 226, 213, 112, 94, 84, 71, 58
DP1	C ₁₈ H ₂₃ N ₄ O ₄ ⁺	359.1714	359.1710	-1.11	314, 289, 244, 216, 178, 112, 94, 84, 71
DP2	C ₂₂ H ₂₁ ClFN ₄ O ₄ ⁺	459.1230	459.1220	-2.18	441, 389, 371, 343, 305, 71
DP3	C ₁₈ H ₁₇ ClFN ₄ O ₂ ⁺	375.1019	375.1011	-2.13	305, 288, 277, 269, 261, 250, 160, 135, 108, 71
DP4	C ₂₄ H ₂₈ ClFN ₅ O ₄ ⁺	504.1808	504.1801	-1.39	486, 459, 441, 389, 375, 371, 305, 130, 112, 94, 84
DP5	C ₂₈ H ₃₀ ClFN ₅ O ₇ ⁺	602.1812	602.1811	-0.17	558, 532, 514, 487, 421, 377, 112, 94, 84, 71
DP6	C ₂₄ H ₂₇ ClN ₅ O ₄ ⁺	484.1746	484.1749	0.62	439, 414, 396, 369, 341, 329, 303, 112, 94, 84
DP7	C ₂₂ H ₁₉ ClFN ₄ O ₃ ⁺	441.1124	441.1124	0.00	371, 343, 304, 288, 71
DP8	C ₂₂ H ₂₁ ClFN ₄ O ₅ ⁺	475.1179	475.1184	1.05	405, 387, 375, 359, 341, 305, 71
DP9	C ₂₄ H ₂₆ ClFN ₅ O ₃ ⁺	486.1703	486.1701	-0.41	441, 429, 416, 398, 375, 371, 359, 343, 331, 317, 305, 288, 226, 213, 112, 94, 84, 71, 58
DP10	C ₁₉ H ₁₇ ClFN ₄ O ₃ ⁺	403.0968	403.0969	-0.25	333, 315, 305, 160
DP11	C ₂₂ H ₁₉ ClFN ₄ O ₄ ⁺	457.1073	457.1077	0.88	387, 369, 359, 341, 272, 242, 71

3.3.1. MS/MS and NMR of AFT dimaleate and DP9

The MS/MS data of [M+H]⁺ ions of AFT and DP9 with an elemental composition of C₂₄H₂₆ClFN₅O₃⁺ and accurate mass *m/z* 486.1701 displays similar fragmentation pattern. The DP9 was observed in photolytic conditions and believed to be the Z-isomer of the drug. The ESI-MS/MS spectrum of [M+H]⁺ ion of protonated AFT (Fig. S3a) (retention time (*t*_R) = 7.4 min.) and DP9 (Fig. S5b) (*t*_R = 7.0 min.) with *m/z* 486 displays characteristic high abundant fragment ion at *m/z* 371 and *m/z* 305 formed by the loss of tetrahydrofuran (from *m/z* 441) and (E)-4-(dimethylamino) but-2-enal (from *m/z* 416), respectively. Further, formation of product

ions at *m/z* 416 and *m/z* 359 with the loss of C₄H₆O from *m/z* 486 and *m/z* 429, respectively confirms the presence of tetrahydrofuran moiety in the drug and DP9. The formation of prominent fragment ion at *m/z* 112 indicates the presence of dimethylamino but-2-enal moiety. Further, structure specific fragment ion at *m/z* 441 formed from AFT/DP9 indicates the presence of terminal dimethylamine group (**Scheme S1**). The formation of product ion at *m/z* 441 can be explained by 'H' migration from the methylene group to the terminal nitrogen followed by dimethylamine loss. The formation of characteristic fragment ions similar to the drug confirms that DP9 to be Z-isomer of AFT. The probable mechanism for the formation of

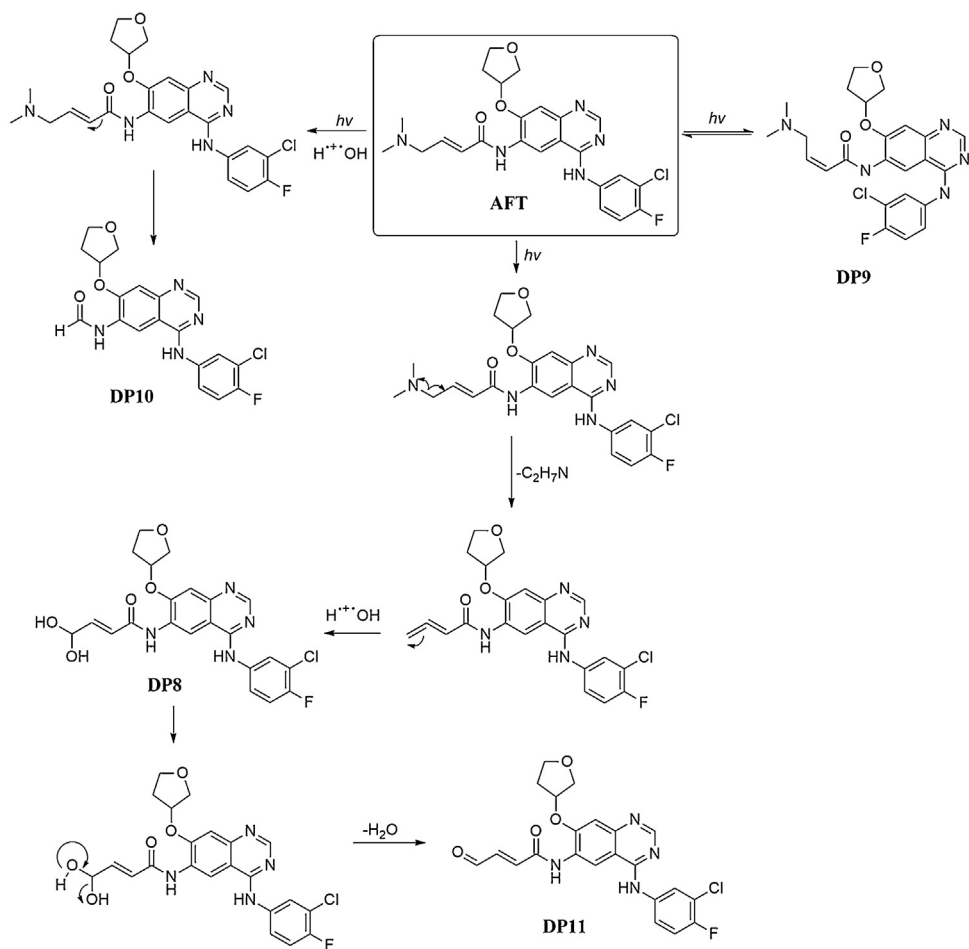
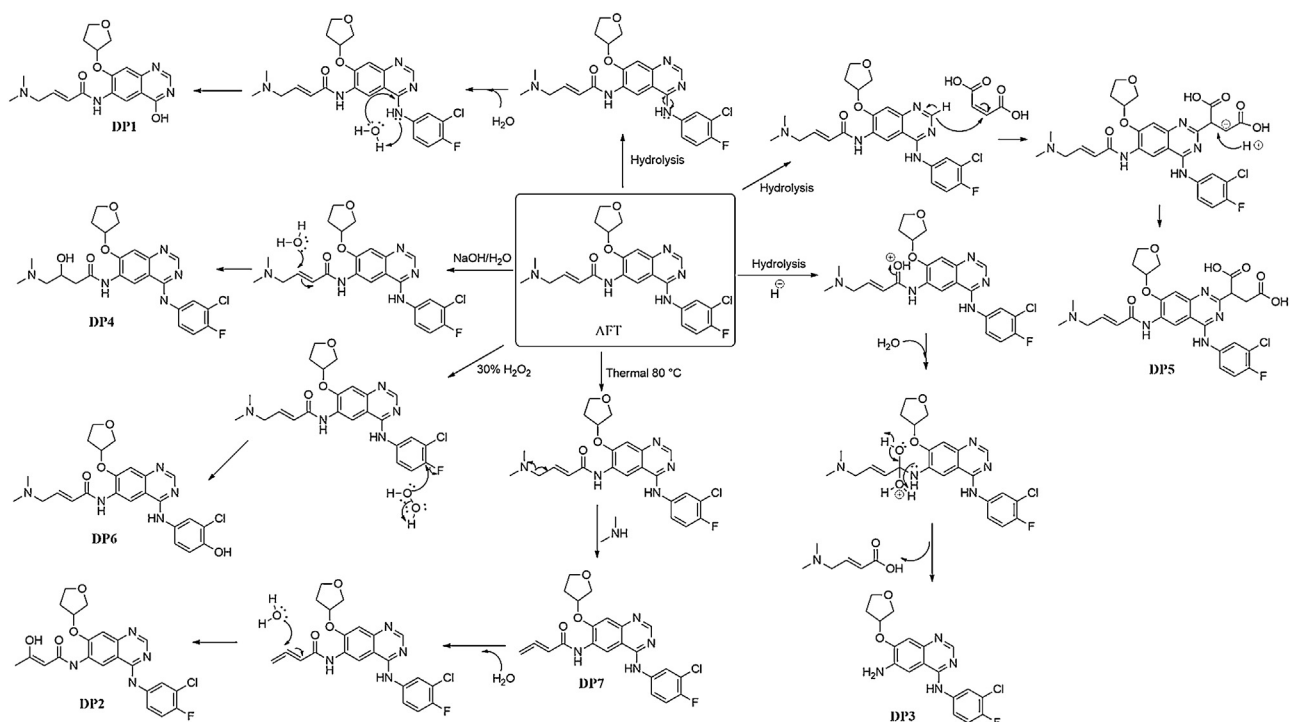
**Scheme 1.** Probable mechanism for the formation of DP8-DP11.**Scheme 2.** Probable mechanism for the formation of DP1-DP7.

Table 2

Table 2 ^1H and ^{13}C NMR assignments for AFT dimaleate and its DPs.

Position	Afatinib dimaleate	DP2	DP3
	δ_H (ppm), Multiplicity	δ_C (ppm)	δ_H (ppm), Multiplicity
1/3	2.83 (s, 6 H)	42.70	–
4	3.84 (m, 2 H)	57.43	2.39 (m, 3 H)
5	6.81 (m, 1 H)	136.99	–
6	6.81 (m, 1 H)	132.19	6.33 (m, 1 H)
7	–	162.90	–
9	10.02 (s, 1 H)	–	–
10	–	133.72	137.10
11	8.59 (s, 1 H)	108.01	8.39 (s, 1 H)
12	–	117.36	109.34
13	–	157.52	7.80 (m, 1 H)
14	9.77 (s, 1 H)	–	123.96
15	–	116.98	–
16	7.28 (s, 1 H)	124.42	157.39
17	–	127.75	9.39 (s, 1 H)
19	7.78 (m, 1 H)	119.26	116.97
20	7.45 (t, 1 H)	123.24	7.31 (d, 1 H)
21	–	152.96	125.71
24	8.96 (s, 1 H)	154.15	7.05 (s, 1 H)
26	–	148.30	127.22
27	8.11 (dd, 1 H)	109.21	7.40 (d, 1 H)
28	–	154.90	119.23
30	5.32 (m, 1 H)	79.48	7.38 (d, 1 H)
31	3.99 (m, 2 H)	72.48	122.76
33	3.99 (m, 2 H)	67.07	152.78
34	2.25 (m, 2 H)	32.08	154.71
35	–	–	8.37 (s, 1 H)
36/39 (dimaleate)	–	167.44	151.49
37/38(dimaleate)	6.15 (s, 4 H)	133.87	8.19 (dd, 1 H)
		–	145.08
		105.37	107.87
		–	154.15
		78.76	5.24 (m, 1 H)
		72.66	3.90 (m, 2 H)
		66.97	3.90 (m, 2 H)
		32.93	2.23 (m, 2 H)
		–	78.53
		–	72.62
		–	67.03
		–	32.97
		–	–
		–	–
		–	–
		–	–
		–	–

s = singlet; d = doublet; t = triplet; m = multiplet; dd = doublet of doublets.

DP9 under photolytic conditions is shown in Scheme 1 [19]. The ^1H and ^{13}C NMR spectra of AFT dimaleate were given in Fig. S6 and S7, respectively (supplementary information). The NMR signals that are structure specific for the AFT dimaleate includes the presence of (E)-4-(dimethylamino)but-2-enamide (atom no. 1, 3, 4, 5, 6, 7 and 9), tetrahydrofuran (atom no. 30, 31, 33 and 34) and dimaleate (atom no. 36, 37, 38 and 39) signals (Table 2). The ^1H and ^{13}C NMR signals of these groups were utilized for the identification of the major DPs (DP2 and DP3).

3.3.2. MS/MS and NMR of degradation products

3.3.2.1. DP1 (m/z 359). The ESI/MS/MS spectra

displays structure indicative product ions at m/z 314 and m/z 244 and absence of drug specific fragment ions (m/z 441, m/z 371 and m/z 305). Also, formation of fragment ions at m/z 112 and m/z 71 indicate that (E)-4-(dimethylamino) but-2-enal and tetrahydrofuran moieties are intact. This clearly suggests the structure of DP1 (Scheme S2). The proposed mechanism for the formation of DP1-DP7 was shown in Scheme 2.

3.3.2.2. DP2 (m/z 459). ESI/MS/MS spectrum of major hydrolytic degradation product DP2 (Fig. S3c) showed the presence of product ion at m/z 305 (as in AFT) and the absence of m/z 112 indicated modification of the side chain (Scheme S3). To confirm the proposed structure of the DP2, NMR (^1H and ^{13}C) studies were carried out. The absence of NMR signals for the dimethylamine group in both proton

(Fig. S8) and carbon (Fig. S9) NMR spectrum of DP2 proved that DP2 was devoid of dimethylamine moiety (Table 2). Further, the presence of ^1H NMR signal of DP2 for the proton at H35 and absence of ^1H NMR signal for the proton at H5 when compared with the drug, confirmed that the DP2 was formed by the hydroxylation at position 5. Additionally, the ^{13}C spectrum of DP2 shows downfield and upfield shift for the carbon at C5 and C6, respectively which demonstrates the hydroxylation at position 5. Based on all these data the structure for the DP2 was identified as shown in Scheme S3.

3.3.2.3. DP3 (m/z 375). ESI/MS/MS spectrum (Fig. S3d) of DP3

showed the characteristic loss of tetrahydrofuran (m/z 70) which leads to formation of structure specific fragment ion at m/z 305. The product ions observed are reported in Scheme S1. The formation of DP3 in hydrolytic conditions can be explained by hydrolytic cleavage of amide bond [20] as shown in Scheme 2. The structure of the DP3 was further established by accurate comparison of NMR signals of AFT and DP3. The NMR study of DP3 showed absence of peaks which correspond to (E)-4-(dimethylamino)but-2-enal in both ^1H (Fig. S10) and ^{13}C NMR (Fig. S11) spectrum compared to drug (Table 2). All these data indicated the structure of DP3 to be N4-(3-chloro-4-fluorophenyl)-7-(tetrahydrofuran-3-yl)oxy quinazoline-4,6-diamine.

3.3.2.4. DP4 (m/z 504). The ESI/MS/MS spectrum of DP4 (Fig. S4a) showed abundant precursor ion peak at m/z 504.1801. Further it

shows loss of water molecule (DP4 to m/z 486 and m/z 130 to m/z 112) and fragment ion at m/z 130 which suggests hydroxylation of the AFT at (E)-4-(dimethylamino)-1-oxobut-2-en-1-ylum side chain. (Scheme S3).

3.3.2.5. DP5 (m/z 602). The ESI/MS/MS spectrum of DP5 (Fig. S4b) showed formation of distinctive product ions including the loss of tetrahydrofuran from DP5, the loss of dimethylamine and C_6H_9NO from m/z 532 and formation of m/z 112 which were in correlation to the product ions formed in the MS/MS of the AFT. All this data demonstrate that DP5 was an adduct of maleic acid with the drug (Scheme S4).

3.3.2.6. DP6 (m/z 484). The molecular formula of the oxidative DP6 ($C_{24}H_{27}ClN_5O_4^+$) indicated an addition of oxygen with the loss of fluorine atom as compared to drug. The ESI/MS/MS spectrum of DP6 (Fig. S4c) showed product ions that correlate to product ions observed in the MS/MS of the AFT. The formation of the ion at m/z 112 indicates that (E)-4-(dimethylamino) but-2-enal moiety was retained (Scheme S5).

3.3.2.7. DP7 (m/z 441). The degradation product DP7 was formed by the loss of dimethylamine from AFT. The MS/MS spectrum of DP7 (Fig. S4d) showed the formation of characteristic product ions as observed in MS/MS spectrum of AFT (Scheme S1).

3.3.2.8. DP8 (m/z 475). The molecular formula of DP8 ($C_{22}H_{21}ClFN_4O_5^+$) indicates an addition of two oxygen atoms with the loss of dimethylamine moiety as compared to the drug. The presence of fragment ion at m/z 375 and absence of characteristic fragment ion of m/z 112 in the MS/MS spectrum (Fig. S5a) of DP8 provide clear evidence of hydroxylation of the drug at the side chain [(E)-4-(dimethylamino) but-2-enal] (Scheme S6). The probable mechanism for the formation of DP8-DP11 was shown in Scheme 1.

3.3.2.9. DP10 (m/z 403). The ESI/MS/MS spectrum of DP10 (Fig. S5c) displayed characteristic loss of tetrahydrofuran (m/z 403 to m/z 333), followed by water loss and CO loss from m/z 333. The loss of CO (m/z 333 to m/z 305) suggests the presence of aldehyde group in the structure of DP10 and the absence of product ion at m/z 112 indicates that DP10 was formed by the loss of N,N-dimethylprop-2-en-1-amine side chain (Scheme S7).

3.3.2.10. DP11 (m/z 457). The ESI/MS/MS spectrum of DP11 ($C_{22}H_{19}ClFN_4O_4^+$) (Fig. S5d) showed presence of structure indicative product ions and the absence of m/z 112 which clearly suggests that DP11 could be formed by the loss of dimethylamine followed by oxidation (Scheme S6).

3.4. In vitro cell viability assay

The DPs (DP2 and DP3) of AFT were evaluated for their cytotoxicity on non small cell lung cancer cell line A549. AFT showed 88.8% inhibition of cell growth, DP2 exerted cytotoxicity by inhibiting 78.3% of the cell growth and DP3 was found to inhibit cell growth by 62.7% in A549 cells at highest screened concentration of $40\mu M$. IC_{50} values of AFT, DP2 and DP3 were found to be 15.02 ± 1.49 , 25.00 ± 1.26 and 32.56 ± 0.11 respectively on A549 cells (Fig. 2) which demonstrates decrease in cytotoxic activity of DPs on A549 cell line as compared to the AFT.

3.5. In silico toxicity studies

The potential toxicity of AFT and its stress DPs were predicted by ProTox-II tool. Different levels of toxicity endpoints such as oral tox-

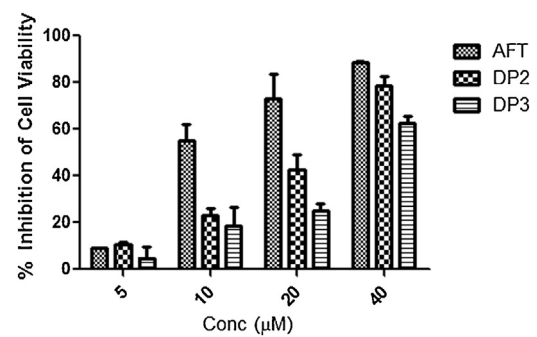


Fig. 2. Cytotoxicity studies of AFT, DP2 and DP3 on non small cell lung cancer cell line A549.

icity, organ toxicity (hepatotoxicity), toxicological endpoints (such as mutagenicity, carcinotoxicity, cytotoxicity and immunotoxicity), toxicological pathways and toxicity targets were incorporated. Different levels of toxicity target helps to provide insight into the most likely possible molecular mechanism behind such toxic response. The predicted outcomes for each target will show by the confidence score. The score below 70% (0.7) is omitted whereas above it where considered as active to the input molecule [21]. The predicted toxicity of different target for AFT and its DPs are shown in the Table S5 (A–B). The predicted toxic dose (LD50) for all the DPs are in the range of $500\text{--}1500\text{ mg kg}^{-1}$ and falls under toxicity class IV, toxic. The toxicological endpoint, immunotoxicity, for DP2 to DP11 is predicted to be active with confidence score >90% whereas confidence score for hepatotoxicity, carcinogenicity, mutagenicity, cytotoxicity and toxicological pathways were <70%. AFT and its DPs showed no binding probability for both toxicological pathways (AhR, AR, AR-LBD, ER, ER-LBD, aromatase, PPAR-Gamma, nrf2/ARE, HSE, MMP, p53, ATAD5) and toxicological targets (Adenosine receptor A2a, Beta-2 adrenergic receptor, Androgen receptor, Amine oxidase A, Corticotropin-releasing factor receptor 1, D(3) dopamine receptor, Estrogen receptor, Estrogen receptor beta, Glucocorticoid receptor, Histamine H1 receptor, Nuclear receptor subfamily 1 group, Kappa-type opioid receptor, Mu-type opioid receptor, cAMP-specific 3, Prostaglandin G/H synthase 1, Nuclear receptor subfamily 3 group C member 3). Thus ProTox-II predicts that there is a possibility that the AFT and its DPs (DP2 and DP11) can be active for immunotoxicity and thereby resulting in severe toxic effect.

4. Conclusion

A selective stability indicating HPLC method was developed to study the degradation behavior of AFT under hydrolytic, oxidative, thermal and photolytic conditions. Stress degradation studies were carried out by examining the factors suggested by ICH guidelines. The drug was found to be degraded in all above studied conditions and results in formation of 11 new hitherto degradation products. All the DPs were identified and characterized using LC-Q-TOF/MS/MS along with molecular formula generation. Structural confirmation was provided for the major DPs (DP2 and DP3) using NMR experiments (1H and ^{13}C). The mechanistic explanation was provided for the formation of each DP. The MTT assay was performed to evaluate the cytotoxicity of the isolated DPs using A549 cell line. Additionally, *in silico* toxicity studies were performed with ProTox-II tool where toxicological endpoint, immunotoxicity of DP2 and DP11 were predicted with high probability score. The developed HPLC method was validated in terms of specificity, linearity, accuracy, precision and robustness. The developed HPLC and LC-MS/MS method can be useful for quality control analysis and detection and characterization of degradation impurities.

Acknowledgements

The authors thank Dr. Shashi Bala Singh, Director, NIPER-Hyderabad, India for facilities and encouragement. Authors BC and SV are grateful to Sun Pharmaceutical Industries Ltd. Vadodara, India for the gift sample of the Afatinib dimaleate. The authors are also thankful to the Department of Pharmaceuticals, Ministry of Chemicals and Fertilizer, New Delhi, India, for providing a Research Fellowship.

Appendix A. Supplementary data

Supplementary material related to this article can be found, in the online version, at doi:<https://doi.org/10.1016/j.jpba.2019.01.004>.

References

- [1] F. Solca, G. Dahl, A. Zoepf, G. Bader, M. Sanderson, C. Klein, O. Kraemer, F. Himmelsbach, E. Haaksma, G.R. Adolf, Target binding properties and cellular activity of afatinib (BIBW 2992), an irreversible ErbB family blocker, *J. Pharmacol. Exp. Ther.* 343 (2) (2012) 342–350.
- [2] D. Li, L. Ambrogio, T. Shimamura, S. Kubo, M. Takahashi, L. Chiriac, R. Padera, G. Shapiro, A. Baum, F. Himmelsbach, BIBW2992, an irreversible EGFR/HER2 inhibitor highly effective in preclinical lung cancer models, *Oncogene* 27 (34) (2008) 4702.
- [3] <https://www.fda.gov/Drugs/InformationOnDrugs/ApprovedDrugs/ucm592558.htm>. (Last Accessed 03 May 2018).
- [4] ICH guideline, Q1A (R2), stability testing of new drug substances and products, International Conference on Harmonisation (2003).
- [5] FDA, Guideline for Submitting Documentation for the Stability of Human Drugs and Biologics, Food and Drug Administration, Rockville, MD, 1987.
- [6] R.W. Sparidans, S. van Hoppe, J.J. Rood, A.H. Schinkel, J.H. Schellens, J.H. Beijnen, Liquid chromatography-tandem mass spectrometric assay for the tyrosine kinase inhibitor afatinib in mouse plasma using salting-out liquid-liquid extraction, *J. Chromatogr. B* 1012 (2016) 118–123.
- [7] H. Hayashi, Y. Kita, H. Iihara, K. Yanase, Y. Ohno, C. Hirose, M. Yamada, K. Todoroki, K. Kitaichi, S. Minatoguchi, Simultaneous and rapid determination of gefitinib, erlotinib and afatinib plasma levels using liquid chromatography/tandem mass spectrometry in patients with non-small-cell lung cancer, *Biomed. Chromatogr.* 30 (7) (2016) 1150–1154.
- [8] M. Fouad, M. Helvenstein, B. Blankert, Ultra high performance liquid chromatography method for the determination of two recently FDA approved TKIs in human plasma using diode array detection, *J. Anal. Methods Chem.* 2015 (2015) 1–6.
- [9] S.X. Xiang, C. Kang, L.X. Xie, X.L. Yin, H.W. Gu, R.Q. Yu, Fast quantitative analysis of four tyrosine kinase inhibitors in different human plasma samples using three-way calibration-assisted liquid chromatography with diode array detection, *J. Sep. Sci.* 38 (16) (2015) 2781–2788.
- [10] D. Schinell, S. Buschke, H. Fuchs, D. Gansser, R.-G. Goeldner, M. Utterreuther-Fischer, P. Stopfer, S. Wind, M. Petersen-Sylla, A. Halabi, Pharmacokinetics of afatinib in subjects with mild or moderate hepatic impairment, *Cancer Chemother. Pharmacol.* 74 (2) (2014) 267–275.
- [11] P. Stopfer, K. Marzin, H. Narjes, D. Gansser, M. Shahidi, M. Utterreuther-Fischer, T. Ebner, Afatinib pharmacokinetics and metabolism after oral administration to healthy male volunteers, *Cancer Chemother. Pharmacol.* 69 (4) (2012) 1051–1061.
- [12] R. Vejjenda, C. Subramanyam, G. Veerabhadram, New RP-HPLC method for the determination of afatinib dimaleate in bulk and pharmaceutical dosage forms, *Indo-Am. J. Pharm. Res.* 4 (2015) 2098–2111.
- [13] B.B. Chavan, P.D. Kalariya, R. Srinivas, M.V.N.K. Talluri, Alcaftadine: selective separation and characterization of degradation products by LC-QTOF-MS/MS, *Chromatographia* 81 (4) (2018) 631–638.
- [14] P.D. Kalariya, M.V.N.K. Talluri, P.N. Patel, R. Srinivas, Identification of hydrolytic and isomeric N-oxide degradants of vilazodone by on line LC-ESI-MS/MS and APCI-MS, *J. Pharm. Biomed. Anal.* 102 (2015) 353–365.
- [15] P.S. Devrukhabar, G. Shankar, R. Srinivas, Proposal of degradation pathway with toxicity prediction for hydrolytic and photolytic degradation products of timolol, *J. Pharm. Biomed. Anal.* 154 (2018) 7–15.
- [16] B.B. Chavan, P. Radhakrishnanand, P.D. Kalariya, M.V.N.K. Talluri, Development of stability indicating UPLC method for terconazole and characterization of acidic and oxidative degradation products by UPLC-Q-TOF/MS/MS and NMR, *New J. Chem.* 42 (2018) 10761–10773.
- [17] ICH Guideline Q2 (R1), Validation of analytical procedures: text and methodology, International Conference on Harmonization (2005).
- [18] ICH Guideline Q1B, Stability testing: photostability testing of new drug substances and products, International Conference on Harmonisation (1996).
- [19] Y. Norikane, N. Tamaoki, Photochemical and thermal cis/trans isomerization of cyclic and noncyclic azobenzene dimers: effect of a cyclic structure on isomerization, *Eur. J. Org. Chem.* 2006 (5) (2006) 1296–1302.
- [20] J. March, Advanced Organic Chemistry, Reactions, Mechanisms, and StructureAdvanced Organic Chemistry, Reactions, Mechanisms, and Structure, John Wiley and Sons, Singapore, 2005, pp. 132.
- [21] P. Banerjee, A.O. Eckert, A.K. Schrey, R. Preissner, ProTox-II: a webserver for the prediction of toxicity of chemicals, *Nucleic Acids Res.* (2018).